

Activity dependent internalization of the glutamate transporter GLT-1 requires calcium entry through the NCX sodium/calcium exchanger

Ignacio Ibáñez^{a,b}, David Bartolomé-Martín^{a,b}, Dolores Piniella^{a,b}, Cecilio Giménez^{a,b}, Francisco Zafra^{a,b,*}

^a Centro de Biología Molecular Severo Ochoa, Facultad de Ciencias, Consejo Superior de Investigaciones Científicas, Universidad Autónoma de Madrid, Madrid, Spain

^b IdiPAZ, Instituto de Salud Carlos III, Madrid, Spain



ARTICLE INFO

Keywords:

Intracellular trafficking
Endocytosis
glutamate
Calcium
Transport

ABSTRACT

GLT-1 is the main glutamate transporter in the brain and its trafficking controls its availability at the cell surface, thereby shaping glutamatergic neurotransmission under physiological and pathological conditions. Extracellular glutamate is known to trigger ubiquitin-dependent GLT-1 internalization from the surface of the cell to the intracellular compartment, yet here we show that internalization also requires the participation of calcium ions. Consistent with previous studies, the addition of glutamate (1 mM) to mixed primary cultures (containing neurons and astrocytes) promotes GLT-1 internalization, an effect that was suppressed in the absence of extracellular Ca^{2+} . The pathways of Ca^{2+} mobilization by astrocytes were analyzed in these mixed cultures using the genetically encoded calcium sensor GCaMP6f. A complex pattern of calcium entry was activated by glutamate, with a dramatic and rapid rise in the intracellular Ca^{2+} concentration partially driven by glutamate transporters, especially in the initial stages after exposure to glutamate. The $\text{Na}^+/\text{Ca}^{2+}$ exchanger (NCX) plays a dominant role in this Ca^{2+} mobilization and its blockade suppresses the glutamate induced internalization of GLT-1, both in astrocytes and in a more straightforward experimental system like HEK293 cells transiently transfected with GLT-1. This regulatory mechanism might be relevant to control the amount of GLT-1 transporter at the cell surface in conditions like ischemia or traumatic brain injury, where extracellular concentrations of glutamate are persistently elevated and they promote rapid Ca^{2+} mobilization.

1. Introduction

The glutamate transporter GLT-1 is responsible for clearing the bulk of extracellular glutamate in the forebrain and although it is mainly found in glial cells, neuronal forms of the transporter also exist (Petr et al., 2015; Tanaka et al., 1997). GLT-1 not only contributes to physiological glutamatergic neurotransmission but it is also responsible for maintaining glutamate below excitotoxic levels, which is critical in pathological conditions like ischemia or traumatic brain injury (Lai et al., 2014). Like many other membrane transporters, GLT-1 trafficking to and from the plasma membrane provides a means to rapidly regulate its activity (Gonzalez and Robinson, 2004; Robinson, 2006). For instance, the major GLT-1 isoform in astrocytes, GLT-1a, displays rapid turnover between the plasma membrane and early endosomes, establishing a dynamic, constitutively cycling pool of transporters that can be rapidly mobilized (Underhill et al., 2015). By contrast, the minor GLT-1 isoform, GLT-1b, is more stably anchored to the membrane through interactions with proteins containing PDZ domains, and it is

mobilized by increases in intracellular calcium and the subsequent activation of CaMKII (Underhill et al., 2015). GLT-1 trafficking can be modulated by glutamate itself, either by promoting its lateral mobility or its internalization from the cell surface (Al Awabdh et al., 2016; Ibanez et al., 2016; Murphy-Royal et al., 2015). This latter process was recently shown to be dependent on the recruitment of arrestin adaptor proteins and the ubiquitin ligase Nedd4-2 (Ibanez et al., 2016). GLT-1 internalization might be particularly relevant to control the levels of extracellular glutamate, which oscillate from micromolar concentrations during basal activity to around 1 mM after neuronal firing (Clements et al., 1992). Actually, these levels may become even higher during ischemic episodes or following traumatic brain injury, pathological situations where the tonic glutamate concentration is raised for several hours, or even days (Nishizawa, 2001). Indeed, GLT-1 is thought to play a central role in the brain responses to fluctuations in glutamate (Mitani and Tanaka, 2003).

Glutamate not only has an impact on neuronal activity but also on glial metabolism. Ca^{2+} is an important mediator in glutamate signaling

* Corresponding author. Centro de Biología Molecular Severo Ochoa, Universidad Autónoma de Madrid, C/ Nicolás Cabrera, 1, 28049, Madrid, Spain.
E-mail address: fzafra@cbm.csic.es (F. Zafra).

to astrocytes, and it has for long been known that glutamate induces waves of free calcium in the astrocyte's cytoplasm and that these frequently propagate between adjacent astrocytes (Cornell-Bell et al., 1990). These calcium oscillations have diverse subcellular localizations, amplitudes and frequencies, and they regulate distinct cellular activities (Bazargani and Attwell, 2016; Shigetomi et al., 2016; Volterra et al., 2014). New calcium sensors (Shigetomi et al., 2010) can now be used to enhance the spatial and temporal resolution when measuring calcium in cells, revealing that spontaneous Ca^{2+} fluctuations in astrocyte processes are mainly driven by the influx of extracellular Ca^{2+} (Shigetomi et al., 2011). However, the mechanism underlying the entry of Ca^{2+} remains unclear and it is possible that multiple channels or transporters are involved (Rungta et al., 2016). Moreover, the contribution of each pathway seems to depend not only on the signaling neurotransmitter but also, on the experimental paradigm and even the Ca^{2+} detection technique employed, often leading to controversial results (see review by (Bazargani and Attwell, 2016).

The glutamate mediated mobilization of Ca^{2+} in astrocytes has been attributed to diverse glutamate receptors, like metabotropic mGluR3 and 5 that promote the efflux of Ca^{2+} from intracellular stores, or ionotropic AMPA and NMDA receptors (AMPA receptors and NMDARs) that promote the entry of extracellular Ca^{2+} (Volterra et al., 2014). Glutamate transporters also play an important role in calcium mobilization by regulating the $\text{Na}^+/\text{Ca}^{2+}$ exchanger (NCX), a bidirectional Na^+ and Ca^{2+} antiporter with a reversal potential close to the resting membrane potential of astrocytes. As such, the NCX can operate in the forward or reverse direction depending on the membrane potential, and the gradients of Na^+ and Ca^{2+} . A glutamate dependent increase in intracellular Na^+ promotes the reverse operation of NCX and it stimulates an increase in intracellular Ca^{2+} (Kirischuk et al., 2007; Rojas et al., 2007). Besides the contribution of NCX to restore the sodium gradient, hampered by glutamate uptake, the increase in Ca^{2+} may underlie the accumulation of mitochondria near glutamate transporters in the astrocytic processes, thereby providing energy to the glutamate transporters (Jackson et al., 2014). Astrocyte processes also experiment transient rises in $[\text{Ca}^{2+}]_i$ that occur independently of synaptic activity, and that are due to the activity of transient receptor potential A1 (TRPA1) channels, which contributes to the resting $[\text{Ca}^{2+}]_i$ (Shigetomi et al., 2011). Interestingly, these channels also collaborate with NCX to regulate mitochondrial mobility in astrocytes (Jackson and Robinson, 2015). Here we show that Ca^{2+} mobilization through NCX channels mediates the glutamate induced internalization of GLT-1, the major glutamate transporter in astrocytes.

2. Materials and methods

2.1. Materials

pGP-CMV-GCaMP6f and pGP-CMV-GCaMP6m were obtained from Addgene (Chen et al., 2013). LckGCaMP6m was generated by transferring the Lck-derived membrane tethering domain from Lck-GCaMP5G in-frame with GCaMP6m. GFAP-GaMP6f was generated by replacing the CMV promoter of pGP-CMV-GCaMP6f with the minimal GFAP promoter by PCR cloning. Z-Link Sulfo-NHS-SS-Biotin was obtained from Pierce and protein standards for sodium dodecyl sulfate-polyacrylamide gel electrophoresis (SDS-PAGE: NZYColour Protein Marker II) were obtained from NZYtech. The TrueFect-Lipo™ and phenylmethanesulfonyl fluoride (PMSF) was purchased from United Biosystems (Rockville, MD), while the nitrocellulose sheets and Clarity™ Western Blot ECL substrate were from Bio-Rad. N-[4-(2-Bromo-4,5-difluorophenoxy)phenyl]-L-asparagine (WAY-213613), 2-Amino-5,6,7,8-tetrahydro-4-(4-methoxyphenyl)-7-(naphthalen-1-yl)-5-oxo-4H-chromene-3-carbonitrile (UCPH-101), (3S)-3-[[3-[[4-(trifluoromethyl)benzoyl]amino]phenyl]methoxy]-L-aspartic acid (TFB-TBOA), N-[(3-aminophenyl) methyl]-6-[4-[(3-fluorophenyl) methoxy] phenoxy]-3-pyridine carboxamide dihydrochloride (YM-244769) and 2-[2-[4-(4-

Nitrobenzyloxy]phenyl]ethyl]isothiourea mesylate (KB-R7943) were purchased from Tocris Bioscience. The monoclonal mouse anti-hemagglutinin (HA: clone 12CA5) was prepared at the microscopy service of the Centro de Biología Molecular (Madrid, Spain), the rabbit anti-MAP2 was from Sigma, the chicken anti-GFAP was from Merck-Millipore (AB5541), the polyclonal guinea pig anti-GLT-1 was from Merck-Millipore (AB1783) and the anti-GLAST antiserum was raised in rats in our laboratory. All other chemicals were obtained from Sigma-Aldrich.

2.2. Primary mixed cultures and immunostaining

Primary mixed cultures were prepared from the cortices of day 17–18 (E17–18) Wistar rat fetuses, as described previously (Brewer, 1995) with minor modifications. The cortex was dissected out and individual cells were disaggregated mechanically in HBSS (Invitrogen) containing 0.25% trypsin (Invitrogen) and 4 mg/ml DNase (Sigma). The cells were plated in poly-D-Lysine coated plates (Falcon) at a density of 1.5×10^6 per 6 cm, and incubated for 4 h in Dulbecco's modified Eagle's medium (DMEM) containing 10% FCS (Fetal Calf Serum), 10 mM glucose, 10 mM sodium pyruvate, 0.5 mM glutamine, 0.05 mg/ml gentamicin, 0.01% streptomycin and 100 $\mu\text{U}/\text{ml}$ penicillin G. Finally, this medium was replaced with Neurobasal/B27 culture medium containing 0.5 mM glutamine. Cytosine arabinoside was not included in the culture medium to allow glial proliferation and the cultured cells were used in the second week after plating. The relative abundance of astrocytes and neurons at this stage was determined by immunostaining of their respective markers, GFAP and MAP2. Immunostaining methods have been previously described (Gonzalez-Gonzalez et al., 2008).

2.3. Cell growth and transfection

HEK293 (American Type Culture Collection) were grown in high glucose DMEM supplemented with 10% FCS at 37 °C in an atmosphere of 5% CO_2 . Transient expression in HEK293 cells was achieved using TrueFect-Lipo according to the manufacturers' instructions. The cells were then incubated for 48 h at 37 °C and then used in biotinylation assays or for electrophysiological recordings.

2.4. Cell surface biotinylation

The non-permeable Sulfo-NHS-SS-Biotin reagent was used for the cell surface biotinylation of HEK293 and primary cultures, after which the biotinylated proteins were isolated and analyzed in western blots as described previously (Jimenez et al., 2011).

2.5. Electrophoresis and immunoblotting

SDS-PAGE was performed on 7.5% polyacrylamide gels in the presence of 2-mercaptoethanol. After electrophoresis, the protein samples were transferred to nitrocellulose membranes for 2 h at $1.2 \text{ mA}/\text{cm}^2$ in a semidry electroblotting system (LKB), using a transfer buffer containing 192 mM glycine and 25 mM Tris-HCl [pH 8.3]. Non-specific binding to the membrane was blocked by incubating the filter for 4 h at 25 °C with 5% non-fat milk protein in 10 mM Tris-HCl (pH 7.5), 150 mM NaCl. The membrane was then probed overnight at 4 °C with the primary antibody (anti-HA, anti-GLT-1 or anti-Calnexin), which was detected after washing with an anti-mouse IgG peroxidase-linked secondary antibody. The proteins detected were visualized by ECL, and quantified by densitometry from films exposed in the linear range on a GS-710 calibrated imaging densitometer (Bio-Rad) and using Quantity One software. Most of the GLT-1 protein was detected as oligomers and these were the bands used for quantification.

2.6. Calcium imaging

Mixed cultures or HEK293 cells were grown in poly-D-Lysine coated

35 mm glass bottom dishes (MatTek) and transfected with plasmids containing either the Ca^{2+} indicator GCaMP6f driven by the GFAP promoter (for astrocytes) or Lck-GCaMP6m driven by the CMV promoter (for HEK293 cells). Lck tag was added to promote the sensor recruitment to the plasma membrane, increasing the sensitivity of the detection in HEK293 cells. HEK293 cells were also co-transfected with a construct containing Cherry-GLT-1 in pCDNA3. Two days after transfection, the cells in the imaging chamber were challenged for 5 min with L-glutamate (1 mM) in aCSF (10 mM HEPES, 140 mM NaCl, 2.4 mM KCl, 2 mM CaCl_2 , 1 mM MgCl_2 , 10 mM glucose [pH7.4]) at 37 °C. For GCaMP imaging, a single optical section was visualized for 5 min at a frequency of 0.2 Hz on a Zeiss AxioVert 200 M, 40Plan Neofluar NA 1.3 objective equipped with an ORCA-Flash4.0 LT CMOS camera. All images were processed and analyzed using FIJI/ImageJ software (Schindelin et al., 2012), background correcting all images. Three ROIs were placed at different membrane regions of the cells to analyze GCaMP6 fluorescence. The fluorescence time course of each cell was measured by averaging all the pixels within the ROIs.

2.7. Electrophysiology

HEK293 cells expressing the HAGLT-1 transporter were grown on 15 mm poly-D-lysine coated coverslips and 48 h after transfection, whole-cell currents were recorded at room temperature (25 °C) in voltage-clamp configuration using a MultiClamp 700 B amplifier (Molecular Devices). Cells were perfused with an extracellular solution containing (in mM) 140 NaCl, 2.4 KCl, 2 CaCl_2 , 1 MgCl_2 , 10 glucose and 10 HEPES [pH 7.4]. Patch recording pipettes (4–6 M Ω) were filled with a solution containing (in mM) 155 potassium gluconate, 4 KCl, 5 MgATP, 0.1 EGTA and 10 HEPES [pH 7.4]. The data were sampled at 20 kHz with a Digidata 1440 A A/D converter (Axon Instruments) and filtered at 4 kHz. HEK293 cells were voltage clamped at -60 mV and cells with a series resistance > 20 M Ω or with more than 20% changes in series resistance during the experiment were discarded. All the data were recorded and analyzed with pCLAMP 10 software (Molecular Devices).

3. Results

We previously showed that the GLT-1 glutamate transporter is internalized from the cell surface to the intracellular compartment by endocytosis, which is triggered by the transporter's own substrate, glutamate, and at concentrations readily attained during ischemic episodes (Ibáñez et al., 2016). This activity-dependent internalization was observed both for the endogenous GLT-1 expressed in primary rat brain cultures (where GLT-1 is mainly localized to astrocytes) and in a heterologous expression system (transfected HEK293 cells), and it was dependent on transporter ubiquitination. Glutamate activates multiple signaling pathways in astrocytes, Ca^{2+} mobilization particularly influencing glial metabolism (Volterra et al., 2014). Therefore, we decided to investigate whether Ca^{2+} might affect the glutamate induced internalization of GLT-1, focusing on mixed primary cultures containing both astrocytes and neurons, and in which neurons were necessary to obtain a robust expression of astrocytic GLT-1 (Gegelashvili et al., 1997). The expression of GLT-1 in individual astrocytes was rather heterogeneous, in contrast with that of GLAST, that stained quite uniformly these cells (Supplemental Fig. S1). The presence of neurons not only activated the synthesis of GLT-1, but also promoted a morphological differentiation of astrocytes (Supplemental Fig. S1).

These primary cultures were stimulated with 1 mM glutamate, in the presence or absence of extracellular Ca^{2+} , and in the presence of NMDAR and AMPAR blockers to avoid neurotoxicity (50 μM APV; 20 μM NBQX). The concentration of transporter at the cell surface was measured in immunoblots after labeling with the non-permeant Sulfo-NHS-biotin reagent. As in our previous studies, the addition of glutamate (1 mM) to the cultures significantly reduced the amount of GLT-1

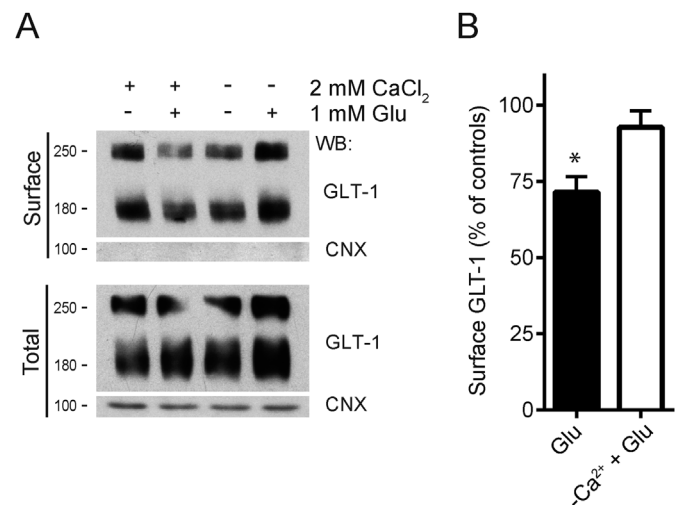
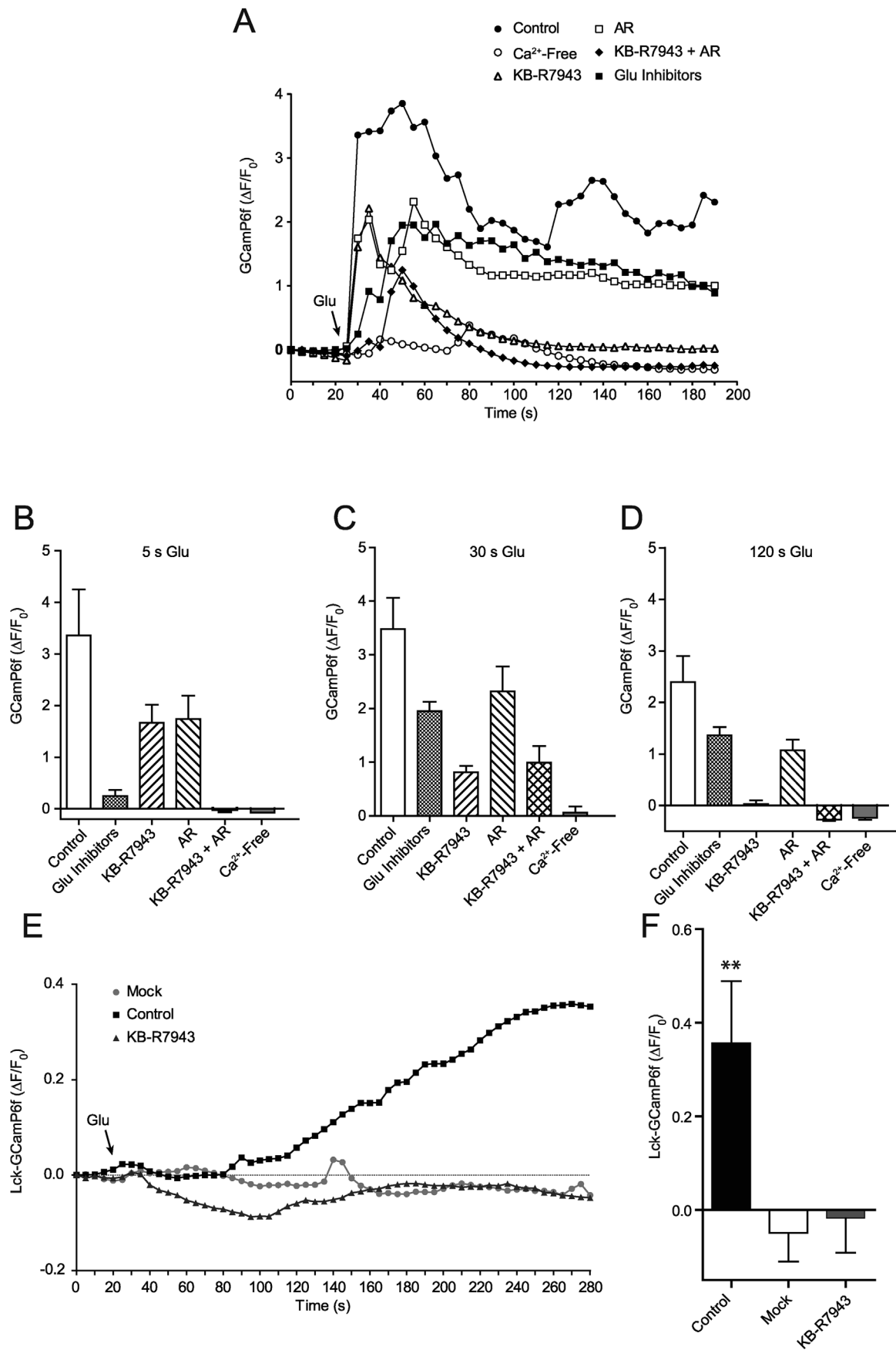


Fig. 1. Calcium dependent internalization of GLT-1 in primary mixed cultures. Rat brain mixed primary cultures were exposed to glutamate (1 mM) for 30 min in the presence or absence of calcium (2 mM CaCl_2). Cell surface proteins were labeled with NHS-Sulfo-biotin and after cell lysis, the biotinylated proteins (surface) were recovered with streptavidin-agarose beads and resolved by SDS-PAGE. Samples of the total cell lysate were run in parallel. GLT-1 expression was analyzed in Western blots and calnexin (CNX) immunodetection was used as a non-biotinylated protein control. The graph in B reflects the densitometric analysis of three independent immunoblots and it represents the mean \pm SEM, normalized to the total GLT-1 expression in each lane, and expressed as percentages of the respective controls (normalized intensities in the absence of glutamate): *, $p < 0.05$ by ANOVA with Bonferroni post-hoc test.

at the cell surface in control aCSF medium. However, this reduction was abolished in a medium that was nominally free of Ca^{2+} , indicating that this process requires Ca^{2+} mobilization (Fig. 1). To determine the dominant calcium source driving GLT-1 internalization and specifically, the contribution of glutamate transporters to calcium mobilization, we transiently transfected the GCaMP6f sensor into cells under the transcriptional control of the GFAP promoter, ensuring it is expressed only in astrocytes. The addition of glutamate elicited a rapid increase in the $[\text{Ca}^{2+}]_i$ to peak F/F_0 values, followed by a slower decline in the signal. However, the amplitude of the initial response and especially, the subsequent decay profiles, were relatively heterogeneous among individual cells (see representative recordings in Supplemental Fig. S2). Hence, the intensity of the Ca^{2+} signals in 12 cells was averaged and represented as a function of time (Fig. 2A).

Pharmacological analysis of the temporal profile of the $\Delta F/F_0$ values revealed a complex source of cytoplasmic Ca^{2+} after the addition of glutamate (Fig. 2 A–D and Supplemental Fig. S2B–E). At very short times, 5 s after glutamate addition (Fig. 2. A, B), most of the $[\text{Ca}^{2+}]_i$ increase required the activity of glutamate transporters as this initial Ca^{2+} response was suppressed by a cocktail of uptake inhibitors (TBOA plus WAY-213613). Both GLT-1 and GLAST contributed to calcium mobilization since inhibition of either GLT-1 (with WAY-213613, 50 μM) or GLAST (with UCPH-101, 50 μM) reduced the $\Delta F/F_0$ values (Supplemental Fig. S3). These inhibitors indicated that the contribution of GLT-1 to total glutamate uptake oscillated between 55 and 60 percent. Moreover, the specific inhibitor of NCXs, KB-R7943, blocked about half of the increase in $[\text{Ca}^{2+}]_i$ and although the source of the other half is more uncertain, it was suppressed by a cocktail of ruthenium red and A967076 (AR in Fig. 2), while it was only partially inhibited by each compound alone (data not shown). This suggests that the TRPA1 channel (which is inhibited by A967076) participates in this process, although other sources cannot be ruled out as ruthenium red also inhibits different TRPs and ryanodine receptors (Clapham et al., 2005; Xu et al., 1999). Nevertheless, this fast response appears to



(caption on next page)

Fig. 2. Changes in intracellular calcium in response to glutamate. A–D. Astrocytes were transfected with GCaMP6f driven by the GFAP promoter. (A) The changes in GCaMP6f fluorescence ($\Delta F/F_0$) were the average obtained from multiple events in several cells ($n = 24–36$ events, 8–12 cells), cells that were tracked for 3 min after the addition of glutamate (1 mM, *arrow*) in the absence (control) or presence of the pharmacological agents indicated: KB-R7943 (10 μ M, KB-R7943); Ruthenium red (20 μ M) + A-967079 (1 μ M) (AR); WAY-213613 (50 μ M) + TBOA (50 μ M), (Glu Inhibitors). Mean peak amplitude of the Ca^{2+} transient ($\Delta F/F_0$) measured in (A) were replotted as histograms at the following times after the application of glutamate: 5 s (B), 30 s (C) and 120 s (D). **E–F.** HEK293 cells were transiently transfected with Lck-GCaMP6m (Mock) or they were co-transfected with Lck-GCaMP6m and mCherry-GLT-1 (Control and KB-R7943). Changes in Lck-GCaMP6m fluorescence were recorded every 5 s for 5 min. Glutamate (1 mM) was added (*arrow*) to cells preincubated in the absence or presence of 10 μ M KB-R7943 (control and KB-R7943, respectively). The graph in E corresponds to the average obtained from multiple events in several cells ($n = 30–36$ events, 8–12 cells). The graph in F corresponds to the statistical analysis of the mean peak amplitude of the Ca^{2+} transient ($\Delta F/F_0$) 4 min after the application of glutamate: **, $p < 0.01$ by ANOVA with Bonferroni post-hoc test.

involve channels activated by ion gradients and the membrane potential over those requiring metabolic activity (i.e., NCX and TRPs over ryanodine receptors).

A little later, after 30 s (Fig. 2A, C), the Ca^{2+} peak reached a maximum and it became partially independent of glutamate transporters as approximately 50% of the rise in calcium was not inhibited by TBOA plus WAY-213613. Nevertheless, this rise was still mainly dependent on calcium entry through NCX, although channels inhibited by the AR cocktail did contribute to the process. Moreover, at this time a transient component became apparent that was resistant to both KB-R7943 and AR, on average responsible for almost one third of the total increase in $[Ca^{2+}]_i$, although not in all cells (see three representative cells in Supplemental Fig. S2E). Later, 2 min after exposure to glutamate (Fig. 2D), the contribution of the glutamate transporter to the rise in calcium continued to diminish, probably due to an increased dependency on signaling pathways activated by glutamate receptors. In terms of calcium channels, NCX remained the dominant source of calcium. Indeed, even the calcium entering at this stage through AR inhibited channels seemed to be dependent on the activity of NCX and it was cancelled by KB-R7943, suggesting a functional coupling between the different calcium channels. Significantly, functional crosstalk between NCX and different TRPs has already been described in other systems (Pulina et al., 2013; Tsumura et al., 2012).

To test whether the coupling between glutamate transporters and NCX is exclusive to astrocytes, we measured $[Ca^{2+}]_i$ in a simpler system where the transporter is internalized from the cell surface in response to glutamate, HEK293 cells transfected with GLT-1 (Ibanez et al., 2016). In these cells, GLT-1 was tagged with the fluorescent Cherry protein and $[Ca^{2+}]_i$ was measured with Lck-GCaMP6f. The response to glutamate was considerably delayed in these cells relative to astrocytes, and it was first observed 90 s after the addition of glutamate, rising steadily over the following 3 min (Fig. 2E). This increase in $[Ca^{2+}]_i$ was dependent on the presence of the transporter since it was not observed in mock transfected cells, and it was suppressed by KB-R7943, indicating it is also coupled to NCX. Together, these data highlight the preponderant role of NCX channels in regulating the intracellular concentration of calcium after exposing astrocytes (in mixed cultures) or GLT-1 transfected HEK293 cells to glutamate, despite the significant differences between both systems. Therefore, we investigated whether NCX also contributed to the glutamate-induced internalization of GLT-1 in these cell types, first challenging mixed primary cultures with glutamate (1 mM) in the presence or absence of the channel inhibitors KB-R7943 or the AR cocktail. Most GLT-1 internalization promoted by glutamate in astrocytes was blocked by KB-R7943, whereas AR did not significantly affect this process (Fig. 3A, C). Another specific inhibitor of NCX (YM-244769, 1 μ M) had a similar inhibitory effect on GLT-1 internalization in astrocytes (Fig. 3B and C). Likewise, the GLT-1 internalization promoted by glutamate in HEK293 cells was prevented by KB-R7943, when assessed by surface biotinylation (Fig. 4A) or by measuring the ion currents associated to GLT-1 activity in electrophysiological recordings (Fig. 4B–E). After setting the voltage at -60 mV, the currents activated by glutamate (1 mM) were measured twice, at $t = 0$ and at $t = 20$ min, perfusing the cells between these measurements with saline solution containing glutamate (1 mM) in the presence or absence of KB-R7943, or with saline alone (control). Before

measuring the current at $t = 20$, the cells were washed until the voltage returned to the basal level. The current induced by glutamate (1 mM) at $t = 20$ min was significantly smaller than that induced at $t = 0$ (Fig. 4C). However, in the presence of KB-R7943 the reduction in the current induced by glutamate at the second time point was not evident, and it may even have been enhanced (Fig. 4E). Together, these studies demonstrate that Ca^{2+} is necessary to induce the glutamate dependent internalization of the transporter.

4. Discussion

We previously reported that the glial glutamate transporter GLT-1 is internalized from the cell surface to the intracellular compartment by endocytosis, which is activated by glutamate, and requires the recruitment of adaptor proteins of the arrestin family, followed by the ubiquitin ligase Nedd4-2. Here we describe that calcium is another player of this process. In astrocytes, Ca^{2+} from intracellular and extracellular compartments is mobilized through calcium channels in response to added or synaptically released glutamate, and regulates diverse aspect of the glial metabolism (Cornell-Bell et al., 1990; Porter and McCarthy, 1996; Volterra et al., 2014). To investigate the relationship between calcium mobilization and the internalization of GLT-1, we have used mixed brain primary cultures since, in this experimental system, astrocytes robustly express GLT-1 due to the presence of neurons. Moreover, the presence of neuronally derived factors promotes a morphological differentiation of astrocytes that includes stellation and emission of diverse types of lamellipodial and filopodial protrusions, assuming a phenotype closer to that exhibited *in situ*. This system is easily accessible to the imaging procedures required for calcium determinations and to the biochemical manipulations used to study GLT-1 trafficking, while displaying morphological and presumably biochemical properties similar to native astrocytes. Since the pathways of calcium mobilization in these cultures were unexplored, we determined the major pathways of calcium entry into the cytoplasm and found that at the very early stages, within second after the addition of glutamate, the cytosolic concentration of calcium increased dramatically due to the own activity of glutamate transporters, GLT-1 and GLAST, both abundantly expressed in this system. This fast response appears to involve channels activated by ion gradients and the membrane potential over those requiring metabolic activity (i.e., NCX and TRPs over ryanodine receptors). At later stages, permeation through NCX became the dominant source of calcium although other sources of calcium were apparent. Relative to the contribution of this mobilized calcium to GLT-1 endocytosis, NCX plays a dominant role and its blockade suppresses the glutamate induced internalization of GLT-1, both in astrocytes and in a more straightforward experimental system like HEK293 cells transiently transfected with GLT-1. These data are consistent with previous studies proposing that NCX underlies the compensatory response of Bergmann glia to the depolarizing entry of sodium through glutamate transporters, and in pure cultures of astrocytes, where depolarization was coupled to Ca^{2+} entry through NCX (Kirischuk et al., 2007; Rojas et al., 2007). The importance of glutamate transporters to the early movement of Ca^{2+} is consistent with data indicating that the transporter mediates sodium entry, while the immediate activation of calcium entry might also be required to trigger

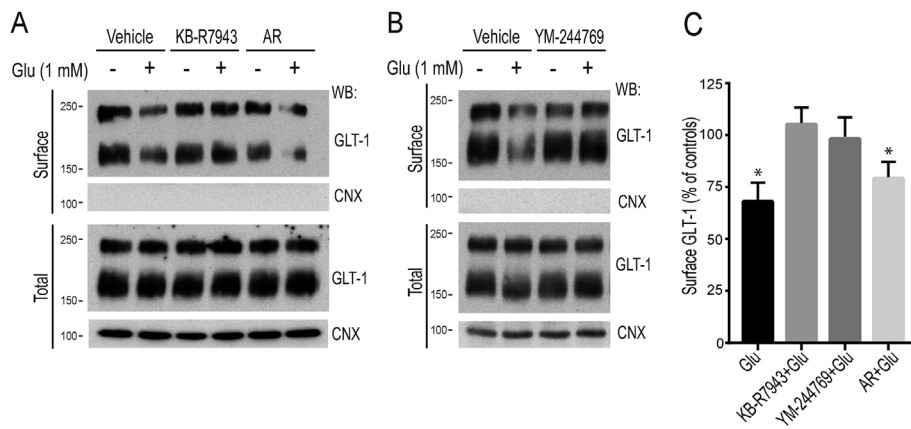


Fig. 3. Role of NCX on glutamate dependent GLT-1 internalization in primary cultures. A–B. Rat brain mixed primary cultures were preincubated for 30 min with 10 μ M KB-R7943 (KB-R7943) or 20 μ M Ruthenium red + 1 μ M A-967079 (AR) (in panel A), or 1 μ M YM-244769 (in panel B), or vehicle and then exposed to 1 mM glutamate for 30 min, as indicated. The cell surface proteins were labeled, isolated and characterized as in Fig. 1. The graph in C corresponds to the densitometric analysis of three independent immunoblots and it represents the mean \pm SEM of the bands, normalized to the total GLT-1 expression in each lane, and expressed as percentages of the respective controls (normalized intensities in the absence of glutamate): *, $p < 0.05$ by ANOVA with Bonferroni post-hoc test.

the first responses of astrocytes to glutamate. For instance, it is known that glutamate induces rapid metabolic changes in astrocytes, such as enhanced glucose capture seconds after exposure to glutamate (Loaiza et al., 2003; Porrás et al., 2008). This stimulation was shown to involve glutamate transporters and it is not mimicked by the activation of AMPA or metabotropic glutamate receptors (Porrás et al., 2008). Similarly, calcium entry through NCX promotes ATP synthesis in the C6 and SH-SY5Y cell lines due to a functional and physical coupling with the major glutamate transporter expressed by these cells, EAAC1/EAAT3 (Magi et al., 2013). Consistent with these observations, our data support a predominant role of NCX in the response of astrocytes to glutamate in the mixed primary culture system. Although there is no evidence for a physical association of GLT-1 and NCX in brain, proteomic studies in brain tissue indicate that both proteins have a common partner, the Na^+/K^+ -ATPase (Genda et al., 2011; Lencesova et al., 2004). Indeed, NCX has been localized to the fine processes of astrocytes where glutamate transporters and Na^+/K^+ -ATPase also concentrate (Chaudhry et al., 1995; Cholet et al., 2002; Minelli et al., 2007; Robinson and Jackson, 2016). The importance of NCX in initiating the internalization of the transporter is maintained even in a simpler heterologous expression system, like HEK293 cells, despite the existence of important kinetic differences. The distinct behavior of astrocytes and HEK293 cells suggests the existence of a much tighter association between glutamate transporters and NCX in astrocytes. Nevertheless, other factors might influence these differences, like the NCX isoform expressed by each cell or the transporter subtype, since astrocytes not only express GLT-1 but also GLAST. Indeed, GLAST might contributed to the observed effects since in our experimental conditions GLAST represents almost half of the total uptake, as estimated by the sensitivity of total uptake to UHP-101, a specific inhibitor of this transporter. Indeed, astrocytes still show transient fluctuations in GCaMP6f fluorescence in the sole presence of the GLT-1 inhibitor WAY-213613.

Internalization of GLT-1 appears to be dependent on recruitment of the ubiquitin ligase Nedd4-2, an interaction mediated by adaptor proteins of the arrestin family (Ibáñez et al., 2016). Indeed, GLT-1 endocytosis might dampen the release of glutamate from astrocytes in a late phase of ischemia when transporters promote glutamate efflux rather than uptake. Thus, the potential cross-talk between the calcium-dependent machinery and ubiquitin-dependent internalization merits further study. Several potential calcium-dependent mechanisms may be activated during ischemia, involving several calcium-dependent kinases. For instance, Protein kinase C might be implicated as it can activate GLT-1 endocytosis through the Nedd4-2 interaction (García-Tardon et al., 2012). AMPK is also activated in ischemia (Li and McCullough, 2010) and it is known to stimulate Nedd4-2 (Bhalla et al., 2006). CamKII is less likely to fulfil an important role in ischemia as it only appears to effect the internalization of GLT-1b, a minor GLT-1 isoform, and not that of the major isoform, GLT-1a (Chawla et al., 2017;

Underhill et al., 2015). Indeed, the CamKII inhibitor CN-93 did not impede the internalization of GLT-1 in astrocytes (data not shown). Calcium itself might directly activate Nedd4-2 which is self-inhibited via intra- or intermolecular C2 and HECT domain interaction. Elevations in intracellular calcium activate Nedd4-2 through binding of Ca^{2+} to the C2 domain and thereby release the C2 domain-mediated self-inhibition (Wang et al., 2010).

Finally, it may be that the calcium-dependent internalization of transporters might be a general response of astrocytes to modulate neuronal activity. Indeed, Ca^{2+} influx into *Drosophila* astrocytes was recently shown to trigger rapid endocytosis of the GABA transporter (GAT) from the plasma membrane, consequently increasing the synaptic GABA that contributes to the neuronal silencing and paralysis observed in these flies (Zhang et al., 2017).

5. Conclusions

In summary, Ca^{2+} mobilization in astrocytes, mainly through the activation of NCX channels, triggers fast responses in astrocytes that provoke the internalization of a fraction of the major glutamate transporter GLT-1. This internalization fine tunes the number of these transporters available at the cell surface, perhaps modulating the activity of neurons in physiological and pathological conditions.

Acknowledgements

We would like to thank E. Núñez and component of SMOC at CBMSO for expert technical help and to Dr. FJ Díez-Guerra for his advice on calcium measurements. This work was supported by grants from the Spanish MINECO (SAF2014- 55686-R) and the “Fundación Ramón Areces”, the latter also providing an institutional grant to CBMSO.

Appendix A. Supplementary data

Supplementary data related to this article can be found at <http://dx.doi.org/10.1016/j.neuint.2018.03.012>.

Fig. S1. Characterization of primary mixed cultures. Primary cultures derived from E17 rat cortices were fixed after 14 days in vitro and processed for immunofluorescence using the indicated antibodies. A. MAP2 and GFAP were used as markers for neurons and astrocytes, respectively. The relative abundance of neurons and astrocytes was quantified in twenty randomly selected fields using the 25 \times objective. Out of 614 immunoreactive cells, 356 were GFAP positive (68%) and 258 (42%) MAP2 positive. B. GLT-1 and GLAST were expressed in astrocytes. Note that while GLAST expression is quite uniform among glial cells (GFAP positive), GLT-1 staining was more heterogeneous. C. GLT-1 is expressed in astrocytes that ensheath neurons (MAP2 positive) that were unstained for this transporter. Scale bar: 50 μ M in A, 45 μ M in B and 15 μ M in C.

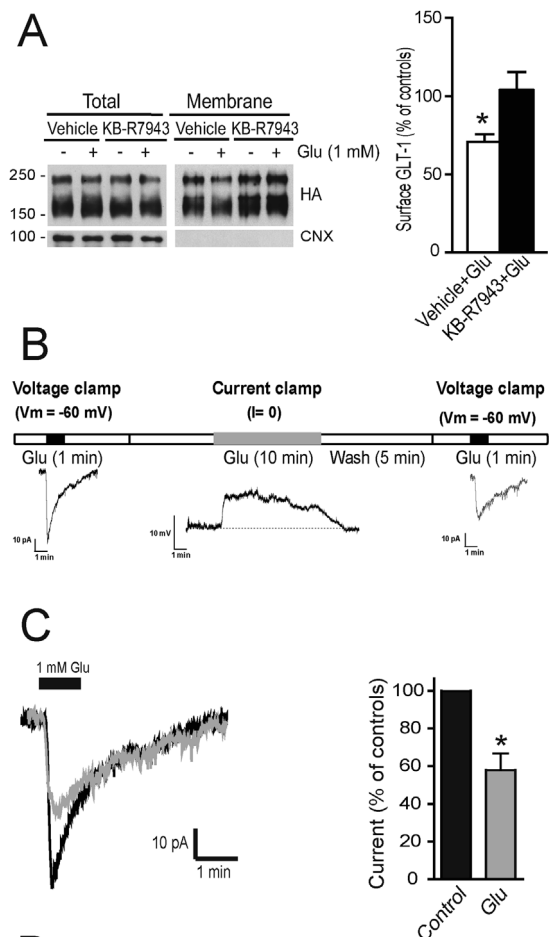


Fig. 4. Role of NCX on glutamate dependent GLT-1 internalization in HEK293 cells. A. HEK293 cells were transiently transfected with HAGLT-1 and 48 h later, the cells were preincubated for 30 min with 10 μ M KB-R7943 (KB-R7943) and then exposed to 1 mM glutamate for 30 min. The cell surface proteins were labeled, isolated and characterized as in Fig. 1. Right panel represents the densitometric analysis of three independent immunoblots, showing the mean intensity \pm SEM of the bands observed in the presence of glutamate, normalized to the total GLT-1 expression in each lane, and expressed as percentages of the respective controls (normalized intensities in the absence of glutamate): *, $p < 0.05$ by ANOVA with Bonferroni post-hoc test.

B-C. HEK293 cells were transiently transfected with HAGLT-1 and 48 h later, the cells were analyzed by patch clamping. (B) Scheme of the experiment. Whole-cell currents were first recorded in voltage-clamp configuration (-60 mV) during a 1 min pulse of glutamate (1 mM) and then, under current clamp conditions, the cells were exposed to glutamate (1 mM) for 10 min. Finally, after washing, the glutamate pulse was repeated in voltage-clamp configuration (-60 mV). (C) The left graph corresponds to representative traces of currents elicited by the glutamate pulses (first pulse, black trace; second pulse gray trace) measured in a single cell, with glutamate present in the current clamp period. The right graph corresponds to average currents of the first pulse (control) and second pulse (Glu) ($n = 5$ cells; *, $p < 0.05$ two-tailed Student's t-test).

D-E. HEK293 cells were transiently transfected with HAGLT-1 and 48 h later, the cells were analyzed by patch clamping. (D) Scheme of the experiment. Whole-cell currents were first recorded in voltage-clamp configuration (-60 mV) during a 1 min pulse of glutamate (1 mM). Subsequently, the cells were maintained in the presence or absence of KB-R7943 (10 μ M, KB-R7943) for 5 min before exposing them to glutamate (1 mM) for 5 min, under current clamp conditions. Finally, after a 5 min wash, the glutamate pulse was repeated in voltage-clamp configuration (-60 mV). (E) The left graphs correspond to representative traces measured in single cells of currents elicited by the glutamate pulses (first pulse, black traces; second pulse, gray traces) measured in a single cell, with glutamate (pale gray) or glutamate plus KB-R7943 (dark gray) present in the current clamp period. The right graph corresponds to average currents of the first pulse (control) and second pulse (Glu and Glu + KB-R7943) ($n = 5$ cells; *, $p < 0.05$ two-tailed Student's t-test).

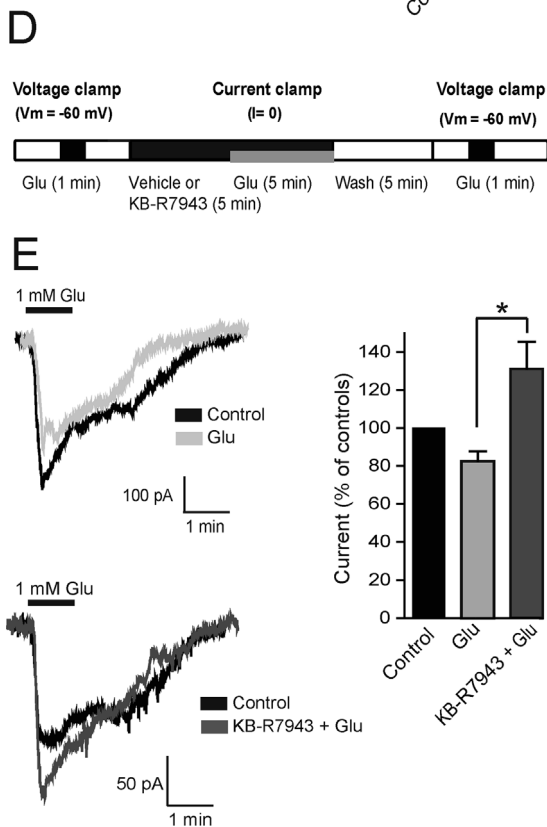


Fig. S2. Intracellular calcium profiles of individual cells. Representative traces from single astrocytes depicting the changes in $[Ca^{2+}]_i$ following application of glutamate (1 mM) in the presence of the pharmacological agents indicated. Astrocytes were transfected with GCaMP6f driven by the GFAP promoter. Each graph represents the changes in $[Ca^{2+}]_i$ of three individual cells following the application of glutamate (1 mM) in the absence or presence of the indicated inhibitors (concentrations, as indicated in Fig. 2).

Fig. S3. Effect of glutamate transporter inhibitors on the intracellular calcium in response to glutamate. Changes in GCaMP6f fluorescence ($\Delta F/F_0$) induced by glutamate 1 mM were determined as in Fig. 2, either in the absence or the presence of WAY-213613 (50 μ M) or UCPH-101 (50 μ M), as indicated in the Figure.

References

Al Awabdh, S., Gupta-Agarwal, S., Sheehan, D.F., Muir, J., Norkett, R., Twelvetrees, A.E., Griffin, L.D., Kittler, J.T., 2016. Neuronal activity mediated regulation of glutamate transporter GLT-1 surface diffusion in rat astrocytes in dissociated and slice cultures. *Glia* 64, 1252–1264.

Bazargani, N., Attwell, D., 2016. Astrocyte calcium signaling: the third wave. *Nat. Neurosci.* 19, 182–189.

Bhalla, V., Oyster, N.M., Fitch, A.C., Wijngaarden, M.A., Neumann, D., Schlattner, U., Pearce, D., Hallows, K.R., 2006. AMP-activated kinase inhibits the epithelial Na^+ channel through functional regulation of the ubiquitin ligase Nedd4-2. *J. Biol. Chem.* 281, 26159–26169.

Brewer, G.J., 1995. Serum-free B27/neurobasal medium supports differentiated growth of neurons from the striatum, substantia nigra, septum, cerebral cortex, cerebellum, and dentate gyrus. *J. Neurosci. Res.* 42, 674–683.

Chaudhry, F.A., Lehre, K.P., van Lookeren Campagne, M., Ottersen, O.P., Danbolt, N.C., Storm-Mathisen, J., 1995. Glutamate transporters in glial plasma membranes: highly differentiated localizations revealed by quantitative ultrastructural immunocytochemistry. *Neuron* 15, 711–720.

Chawla, A.R., Johnson, D.E., Zybura, A.S., Leeds, B.P., Nelson, R.M., Hudmon, A., 2017. Constitutive regulation of the glutamate/aspartate transporter EAAT1 by calcium-

- calmodulin-dependent protein kinase II. *J. Neurochem.* 140, 421–434.
- Chen, T.W., Wardill, T.J., Sun, Y., Pulver, S.R., Renninger, S.L., Baohan, A., Schreier, E.R., Kerr, R.A., Orger, M.B., Jayaraman, V., Looger, L.L., Svoboda, K., Kim, D.S., 2013. Ultrasensitive fluorescent proteins for imaging neuronal activity. *Nature* 499, 295–300.
- Cholet, N., Pellerin, L., Magistretti, P.J., Hamel, E., 2002. Similar perisynaptic glial localization for the Na⁺,K⁺-ATPase alpha 2 subunit and the glutamate transporters GLAST and GLT-1 in the rat somatosensory cortex. *Cerebr. Cortex* 12, 515–525.
- Clapham, D.E., Julius, D., Montell, C., Schultz, G., 2005. International Union of Pharmacology. XLIX. Nomenclature and structure-function relationships of transient receptor potential channels. *Pharmacol. Rev.* 57, 427–450.
- Clements, J.D., Lester, R.A., Tong, G., Jahr, C.E., Westbrook, G.L., 1992. The time course of glutamate in the synaptic cleft. *Science* 258, 1498–1501.
- Cornell-Bell, A.H., Finkbeiner, S.M., Cooper, M.S., Smith, S.J., 1990. Glutamate induces calcium waves in cultured astrocytes: long-range glial signaling. *Science* 247, 470–473.
- García-Tardon, N., Gonzalez-Gonzalez, I.M., Martínez-Villarreal, J., Fernández-Sánchez, E., Gimenez, C., Zafra, F., 2012. Protein kinase C (PKC)-promoted endocytosis of glutamate transporter GLT-1 requires ubiquitin ligase Nedd4-2-dependent ubiquitination but not phosphorylation. *J. Biol. Chem.* 287, 19177–19187.
- Gegelashvili, G., Danbolt, N.C., Schousboe, A., 1997. Neuronal soluble factors differentially regulate the expression of the GLT1 and GLAST glutamate transporters in cultured astroglia. *J. Neurochem.* 69, 2612–2615.
- Genda, E.N., Jackson, J.G., Sheldon, A.L., Locke, S.F., Greco, T.M., O'Donnell, J.C., Spruce, L.A., Xiao, R., Guo, W., Putt, M., Seeholzer, S., Ischiropoulos, H., Robinson, M.B., 2011. Co-compartmentalization of the astroglial glutamate transporter, GLT-1, with glycolytic enzymes and mitochondria. *J. Neurosci.* 31, 18275–18288.
- Gonzalez-Gonzalez, I.M., García-Tardon, N., Cubelos, B., Gimenez, C., Zafra, F., 2008. The glutamate transporter GLT1b interacts with the scaffold protein PSD-95. *J. Neurochem.* 105, 1834–1848.
- Gonzalez, M.I., Robinson, M.B., 2004. Neurotransmitter transporters: why dance with so many partners? *Curr. Opin. Pharmacol.* 4, 30–35.
- Ibáñez, I., Díez-Guerra, F.J., Gimenez, C., Zafra, F., 2016. Activity dependent internalization of the glutamate transporter GLT-1 mediated by beta-arrestin 1 and ubiquitination. *Neuropharmacology* 107, 376–386.
- Jackson, J.G., O'Donnell, J.C., Takano, H., Coulter, D.A., Robinson, M.B., 2014. Neuronal activity and glutamate uptake decrease mitochondrial mobility in astrocytes and position mitochondria near glutamate transporters. *J. Neurosci.* 34, 1613–1624.
- Jackson, J.G., Robinson, M.B., 2015. Reciprocal regulation of mitochondrial dynamics and calcium signaling in astrocyte processes. *J. Neurosci.* 35, 15199–15213.
- Jimenez, E., Zafra, F., Perez-Sen, R., Delicado, E.G., Miras-Portugal, M.T., Aragon, C., Lopez-Corcuera, B., 2011. P2Y purinergic regulation of the glycine neurotransmitter transporters. *J. Biol. Chem.* 286, 10712–10724.
- Kirischuk, S., Kettenmann, H., Verkhratsky, A., 2007. Membrane currents and cytoplasmic sodium transients generated by glutamate transport in Bergmann glial cells. *Pflügers Archiv* 454, 245–252.
- Lai, T.W., Zhang, S., Wang, Y.T., 2014. Excitotoxicity and stroke: identifying novel targets for neuroprotection. *Prog. Neurobiol.* 115, 157–188.
- Lenceseva, L., O'Neill, A., Resneck, W.G., Bloch, R.J., Blaustein, M.P., 2004. Plasma membrane-cytoskeleton-endoplasmic reticulum complexes in neurons and astrocytes. *J. Biol. Chem.* 279, 2885–2893.
- Li, J., McCullough, L.D., 2010. Effects of AMP-activated protein kinase in cerebral ischemia. *J. Cerebr. Blood Flow Metabol.* 30, 480–492.
- Loaiza, A., Porras, O.H., Barros, L.F., 2003. Glutamate triggers rapid glucose transport stimulation in astrocytes as evidenced by real-time confocal microscopy. *J. Neurosci.* 23, 7337–7342.
- Magi, S., Arcangeli, S., Castaldo, P., Nasti, A.A., Berrino, L., Piegari, E., Bernardini, R., Amoroso, S., Lariccia, V., 2013. Glutamate-induced ATP synthesis: relationship between plasma membrane Na⁺/Ca²⁺ exchanger and excitatory amino acid transporters in brain and heart cell models. *Mol. Pharmacol.* 84, 603–614.
- Minelli, A., Castaldo, P., Gobbi, P., Salucci, S., Magi, S., Amoroso, S., 2007. Cellular and subcellular localization of Na⁺-Ca²⁺ exchanger protein isoforms, NCX1, NCX2, and NCX3 in cerebral cortex and hippocampus of adult rat. *Cell Calcium* 41, 221–234.
- Mitani, A., Tanaka, K., 2003. Functional changes of glial glutamate transporter GLT-1 during ischemia: an in vivo study in the hippocampal CA1 of normal mice and mutant mice lacking GLT-1. *J. Neurosci.* 23, 7176–7182.
- Murphy-Royal, C., Dupuis, J.P., Varela, J.A., Panatier, A., Pinson, B., Baufreton, J., Groc, L., Oliet, S.H., 2015. Surface diffusion of astrocytic glutamate transporters shapes synaptic transmission. *Nat. Neurosci.* 18, 219–226.
- Nishizawa, Y., 2001. Glutamate release and neuronal damage in ischemia. *Life Sci.* 69, 369–381.
- Petr, G.T., Sun, Y., Frederick, N.M., Zhou, Y., Dhamne, S.C., Hameed, M.Q., Miranda, C., Bedoya, E.A., Fischer, K.D., Armsen, W., Wang, J., Danbolt, N.C., Rotenberg, A., Aoki, C.J., Rosenberg, P.A., 2015. Conditional deletion of the glutamate transporter GLT-1 reveals that astrocytic GLT-1 protects against fatal epilepsy while neuronal GLT-1 contributes significantly to glutamate uptake into synaptosomes. *J. Neurosci.* 35, 5187–5201.
- Porras, O.H., Ruminot, I., Loaiza, A., Barros, L.F., 2008. Na⁺(+)-Ca²⁺(+) cosignaling in the stimulation of the glucose transporter GLUT1 in cultured astrocytes. *Glia* 56, 59–68.
- Porter, J.T., McCarthy, K.D., 1996. Hippocampal astrocytes in situ respond to glutamate released from synaptic terminals. *J. Neurosci.* 16, 5073–5081.
- Pulina, M.V., Zulian, A., Baryshnikov, S.G., Linde, C.I., Karashima, E., Hamlyn, J.M., Ferrari, P., Blaustein, M.P., Golovina, V.A., 2013. Cross talk between plasma membrane Na⁺/Ca²⁺ exchanger-1 and TRPC/Orai-containing channels: key players in arterial hypertension. *Adv. Exp. Med. Biol.* 961, 365–374.
- Robinson, M.B., 2006. Acute regulation of sodium-dependent glutamate transporters: a focus on constitutive and regulated trafficking. *Handb. Exp. Pharmacol.* 251–275.
- Robinson, M.B., Jackson, J.G., 2016. Astroglial glutamate transporters coordinate excitatory signaling and brain energetics. *Neurochem. Int.* 98, 56–71.
- Rojas, H., Colina, C., Ramos, M., Benaim, G., Jaffe, E.H., Caputo, C., DiPolo, R., 2007. Na⁺ entry via glutamate transporter activates the reverse Na⁺/Ca²⁺ exchange and triggers Ca²⁺-induced Ca²⁺ release in rat cerebellar Type-1 astrocytes. *J. Neurochem.* 100, 1188–1202.
- Rungta, R.L., Bernier, L.P., Dissing-Olesen, L., Groten, C.J., LeDue, J.M., Ko, R., Drissler, S., MacVicar, B.A., 2016. Ca²⁺ transients in astrocyte fine processes occur via Ca²⁺ influx in the adult mouse hippocampus. *Glia* 64, 2093–2103.
- Schindelin, J., Arganda-Carreras, I., Frise, E., Kaynig, V., Longair, M., Pietzsch, T., Preibisch, S., Rueden, C., Saalfeld, S., Schmid, B., Tinevez, J.Y., White, D.J., Hartenstein, V., Eliceiri, K., Tomancak, P., Cardona, A., 2012. Fiji: an open-source platform for biological-image analysis. *Br. J. Pharmacol.* 9, 676–682.
- Shigetomi, E., Kracun, S., Sofroniew, M.V., Khakh, B.S., 2010. A genetically targeted optical sensor to monitor calcium signals in astrocyte processes. *Nat. Neurosci.* 13, 759–766.
- Shigetomi, E., Patel, S., Khakh, B.S., 2016. Probing the complexities of astrocyte calcium signaling. *Trends Cell Biol.* 26, 300–312.
- Shigetomi, E., Tong, X., Kwan, K.Y., Corey, D.P., Khakh, B.S., 2011. TRPA1 channels regulate astrocyte resting calcium and inhibitory synapse efficacy through GAT-3. *Nat. Neurosci.* 15, 70–80.
- Tanaka, K., Watase, K., Manabe, T., Yamada, K., Watanabe, M., Takahashi, K., Iwama, H., Nishikawa, T., Ichihara, N., Kikuchi, T., Okuyama, S., Kawashima, N., Hori, S., Takimoto, M., Wada, K., 1997. Epilepsy and exacerbation of brain injury in mice lacking the glutamate transporter GLT-1. *Science* 276, 1699–1702.
- Tsumura, M., Sobhan, U., Muramatsu, T., Sato, M., Ichikawa, H., Sahara, Y., Tazaki, M., Shibukawa, Y., 2012. TRPV1-mediated calcium signal couples with cannabinoid receptors and sodium-calcium exchangers in rat odontoblasts. *Cell Calcium* 52, 124–136.
- Underhill, S.M., Wheeler, D.S., Amara, S.G., 2015. Differential regulation of two isoforms of the glial glutamate transporter EAAT2 by DLG1 and CaMKII. *J. Neurosci.* 35, 5260–5270.
- Volterra, A., Liaudet, N., Savtchouk, I., 2014. Astrocyte Ca²⁺(+) signalling: an unexpected complexity. *Nat. Rev. Neurosci.* 15, 327–335.
- Wang, J., Peng, Q., Lin, Q., Childress, C., Carey, D., Yang, W., 2010. Calcium activates Nedd4 E3 ubiquitin ligases by releasing the C2 domain-mediated auto-inhibition. *J. Biol. Chem.* 285, 12279–12288.
- Xu, L., Tripathy, A., Pasek, D.A., Meissner, G., 1999. Ruthenium red modifies the cardiac and skeletal muscle Ca²⁺ release channels (ryanodine receptors) by multiple mechanisms. *J. Biol. Chem.* 274, 32680–32691.
- Zhang, Y.V., Ormerod, K.G., Littleton, J.T., 2017. Astrocyte Ca²⁺ influx negatively regulates neuronal activity. *eNeuro* 4.